PACS numbers: 42.25.Fx; 42.30.Ms; 42.30.Rx
DOI: 10.1070/QE2015v045n10ABEH015560

Spatial correlations and probability density function of the phase difference in a developed speckle-field: numerical and natural experiments

N.Yu. Mysina, L.A. Maksimova, B.B. Gorbatenko, V.P. Ryabukho

Abstract. **Investigated are statistical properties of the phase difference of oscillations in speckle-fields at two points in the far-field diffraction region, with different shapes of the scatterer aperture. Statistical and spatial nonuniformity of the probability density function of the field phase difference is established. Numerical experiments show that, for the speckle-fields with an oscillating alternating-sign transverse correlation function, a significant nonuniformity of the probability density function of the phase difference in the correlation region of the field complex amplitude, with the most probable values 0 and π, is observed. A natural statistical interference experiment using Young diagrams has confirmed the results of numerical experiments.**

Keywords: *speckle-field, speckle-modulation, phase distribution, probability density function of phase difference, diffraction, autocorrelation function, Fourier transform, speckle pattern.*

1. Introduction

In coherent optical systems with scatterer, speckle-modulated optical fields are formed as a result of interference of scattered waves [1–7]. Random arrangement of scattering centres and random phase shifts in the waves scattered by these centres determine the random values of the amplitude and phase of a resultant interference field, i.e., the speckle-field. Such fields arise in recording optical holograms of objects with scattering surfaces [8, 9], in implementation of methods of speckle photography [3–6] and laser interferometry of diffusively scattering objects and media [4–6, 10, 11], as well as of methods of speckle-interferometry in optical astronomy [12, 13] and also in systems of wavefront reconstruction [14] and forming images of scattering objects [15, 16], including the system of human visual perception [17].

Developed diffraction speckle-fields are formed at the phase shifts of scattered waves in the interval $[-\pi, \pi]$ and greater. The complex amplitude at any point of a developed speckle-field within the diffraction zone has a Gaussian statistics [18], while the oscillation phase has a uniform probability density function in the interval $[-\pi, \pi]$ [1, 2, 19, 20].

Spatial transverse phase distribution of the speckle-field has deterministic and stochastic components. The deterministic component is determined by the configuration of the optical system intended for speckle-field formation and observation, including the effect of the scheme's optical elements. It is assumed that the stochastic component of the phase within an individual field speckle remains virtually invariable, while, in transition to a neighbouring speckle, the phase is changed with equal probability by a random value in the range $[-\pi, \pi]$. In other words, the stochastic component of the phase difference $\Delta\varphi(P_1, P_2)$ at the points P_1 and P_2 of the speckle-field, which fall into the neighbouring speckles of the field, is equiprobably distributed within the interval $[-\pi, \pi]$.

In the general case, as shown by our experiments, for the sources of scattered coherent field with a scatterer aperture of arbitrary shape, this representation is valid. However, the authors of [21–25] have shown that, when using a scatterer with a symmetric aperture as a speckle-field source, a statistically nonuniform phase difference distribution of the field in the neighbouring speckles is observed in the far diffraction zone. For the field phase difference at the points which mostly fall into a single speckle, there exists a maximum of the probability density for $\Delta\varphi = 0$. This is expectable, since the stochastic component of the phase spatial distribution within a single speckle remains invariable. However, for the field phase difference at the points that mainly fall into the neighbouring speckles, the maxima of the probability density function for $\Delta\varphi = \pm\pi$ are clearly distinguishable in the experiment. In [25], these statistical regularities are revealed by means of a numerical experiment for the scatterers with apertures of different shapes.

We believe that the reason for the nonuniformity of the statistical distribution of the phase difference in a diffraction speckle-field with maxima for $\Delta\varphi = \pm\pi$ is due to peculiarities of spatial correlation properties of the speckle-field. In the formation of speckle-fields with transverse correlation properties which determine the alternating-sign correlation field function, spatial variation in the probability density function of the field phase difference must be nonuniform, with maxima for $\Delta\varphi = 0$ or $\pm\pi$, depending on the distance between the field points within its correlation region, the size of which may exceed the size of an individual speckle. In [25], the relationship between the correlation properties of the speckle-field and the probability density function of the phase difference has been confirmed.

The objective of this work is to establish the properties of spatial changes in the probability density function of the phase difference in a developed speckle-field in the far-field

N.Yu. Mysina, L.A. Maksimova, V.P. Ryabukho Institute of Precision Mechanics and Control, Russian Academy of Sciences, ul. Rabochaya 24, 410028 Saratov, Russia; N.G. Chernyshevsky Saratov State University, ul. Astrakhanskaya 83, 410012 Saratov, Russia; e-mail: MaksimovaLA@yandex.ru, rvp-optics@yandex.ru;
B.B. Gorbatenko Institute of Precision Mechanics and Control, Russian Academy of Sciences, ul. Rabochaya 24, 410028 Saratov, Russia; Yuri Gagarin State Technical University of Saratov, ul. Polytechnicheskaya 77, 410054 Saratov, Russia

Received 16 May 2014; revision received 9 December 2014
Kvantovaya Elektronika **45** (10) 979–988 (2015)
Translated by M.A. Monastyrskiy

diffraction region and to reveal a relationship between these changes and transverse correlation properties of the field.

2. Correlation properties of speckle fields in the far-field diffraction region

Correlation properties of a scattered field in the far-field diffraction region depend on the distribution of the mean field intensity on the scatterer surface [2, 18]. The size and shape of the scatterer aperture exert a significant effect on the mean intensity distribution, and hence on the correlation properties of the field. The spatial transverse correlation function of the complex amplitude of the speckle field in the far-field diffraction region can be determined by means of the Van Cittert–Zernike theorem as a Fourier transform of the distribution of mean field intensity from the δ-correlated source [1, 2, 18, 26]. In the case of a symmetrical distribution of the field mean intensity and symmetrical source aperture, the correlation function of the diffraction field represents a real-valued function, which, in the general case, follows from the properties of the Fourier transforms [27]. Moreover, under these conditions the correlation function takes the real and alternating-sign oscillating values with abrupt changes in the field mean intensity at the source aperture edges. In particular, the correlation functions $G(\Delta\xi,\Delta\eta)$ ($\Delta\xi,\Delta\eta$ are the differences in spatial coordinates in the diffraction speckle-modulated field) of the diffraction speckle-field generated by the sources having a uniform spatial distribution of the mean radiation intensity and a symmetrical aperture in the form of a square and an annular square (Figs 1a, b) can be written in the analytical form [27]:

$$G_1(\Delta\xi,\Delta\eta) = a^2\operatorname{sinc}(\pi a\Delta\xi)\operatorname{sinc}(\pi a\Delta\eta),$$
$$G_2(\Delta\xi,\Delta\eta) = a^2\operatorname{sinc}(\pi a\Delta\xi)\operatorname{sinc}(a\Delta\eta) - b^2\operatorname{sinc}(\pi b\Delta\xi)\operatorname{sinc}(\pi b\Delta\eta), \qquad (1)$$

where a and b are the dimensions of the source apertures shown in Fig. 1. In Fig. 2, for the normalised correlation functions [curves (2, 3, 4)] constructed for annular squares with different widths of the annular region, we can observe a marked increase in the amplitude of the alternating-sign oscillations when decreasing width $(a-b)/2$ of the annular region.

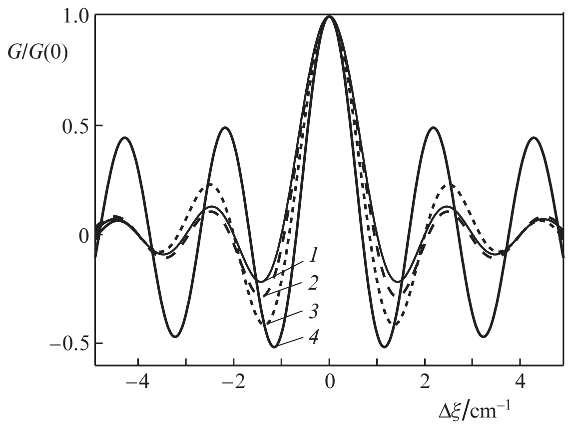

Figure 2. Normalised correlation functions of the complex speckle-field amplitude at $\Delta\eta = 0$ for the sources with apertures in the form of a square with a = 10 mm (*1*) and an annular square with the ratio a/b equal to (*2*) 4, (*3*) 2 and (*4*) 4/3.

In the case of asymmetric shape of the source aperture, the diffraction correlation function may have no alternating-sign oscillations at all, or may have small oscillations. For example, for the field correlation functions in the far-field diffraction region, in the case of source apertures having the shape of a regular triangle and an annular regular triangle, the following expression can be obtained:

$$G_3(\Delta\xi) = \sqrt{3}\left(\frac{a}{2}\right)^2\operatorname{sinc}^2\left(\pi\frac{a}{2}\Delta\xi\right),$$
$$G_4(\Delta\xi) = \sqrt{3}\left(\frac{a}{2}\right)^2\operatorname{sinc}^2\left(\pi\frac{a}{2}\Delta\xi\right) - \sqrt{3}\left(\frac{b}{2}-h\right)^2\operatorname{sinc}^2\left[\pi\left(\frac{b}{2}-h\right)\Delta\xi\right], \qquad (2)$$

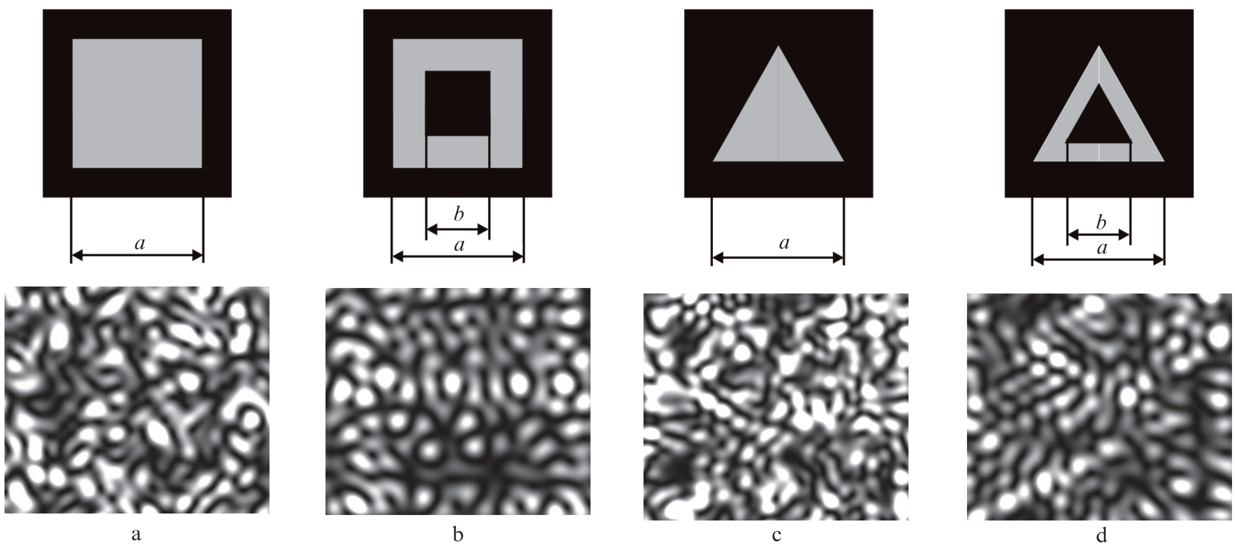

Figure 1. Apertures of scatterers – sources of speckle-fields – and the fragments of simulated speckle patterns generated by such sources with the apertures having the form of (a) square, (b) annular square, (c) triangle and (d) annular triangle.

where $h = (a - b)/2\sqrt{3}$ is the width of the annular region. The normalised correlation functions of the speckle-fields for the sources with such apertures are shown in Fig. 3. If the source has an aperture in the form of a triangle (Fig. 1c), the field correlation function has constant-sign oscillations [Fig. 3, curve (*1*)]. In the case of an annular aperture in the form of a triangle (Fig. 1d), moderate alternating-sign oscillations occur, the amplitudes of which increase with decreasing annular aperture width [Fig. 3, curves (*2*–*4*)].

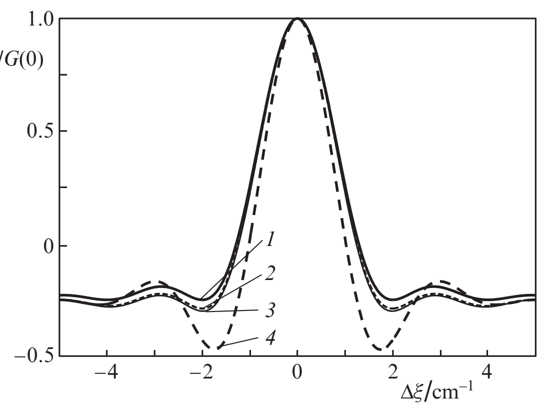

Figure 3. Normalised correlation functions of the complex speckle-field amplitude at $\Delta\eta = 0$ for the sources with apertures in the form of a triangle with a = 10 mm (*1*) and an annular triangle with the ratio a/b equal to (*2*) 4, (*3*) 2 and (*4*) 4/3.

From the physical viewpoint, the correlation properties of a diffraction speckle-field, described by its correlation function, can be explained in terms of wave diffraction on the scatterer aperture representing a speckle-field source. The diffraction field can be represented as a superposition of elementary fields arising in diffraction of planar waves on the scatterer aperture (or, in general case, spherical waves converging in the observation plane of the field diffraction pattern). These elementary diffraction fields constitute a thin amplitude–phase structure of the resulting diffraction field and actually determine its correlation properties [28]. The transverse size $\varepsilon_\perp$ of the field speckles, virtually coinciding with the field's transverse correlation length, is approximately equal to the width of the central maximum of the elementary diffraction field. This view is confirmed, in particular, by the coincidence of integral expressions used to determine the complex amplitude of the elementary diffraction field and the transverse correlation function of the diffraction field defined on the basis of the Van Cittert–Zernike theorem. In the case of symmetric apertures, these elementary diffraction fields are described by real-valued sign-alternating functions and, as a consequence, the correlation function also takes the real-valued sign-alternating values.

3. Numerical experiment to determine the spatial probability density function of the phase difference in the diffraction speckle-field

We performed a numerical statistical experiment to determine the spatial probability density function of the phase difference in the far-field diffraction region of the speckle-field. In this experiment, the probability density of the phase difference $p(\Delta\varphi, \Delta\xi)$ was determined graphically versus the phase difference $\Delta\varphi$ in the range of $[-\pi, \pi]$ and the difference in spatial coordinates $\Delta\xi$ in the speckle-modulated diffraction field. A scheme of the natural experiment being equivalent to the procedure of numerical experiment is presented in Fig. 4.

The field source of a diffraction speckle-modulated field was simulated according to the following algorithm. Two matrices of random independent real values u_{kj} and v_{kj}, distributed in the interval from –1 to +1 in accordance with the normal law, are generated. On their basis, a matrix of random complex variables $U_0(k,j) = u_{kj} + iv_{kj}$ is formed, which creates a random, pixel-by-pixel-correlated Gaussian field of complex variables [18]. This field is modulated by a binary aperture function $P(k,j)$ of a certain form, equal to unity within the aperture and to zero outside it. The complex amplitude distribution of the field source is specified in the form of a discrete array of independent complex random Gaussian variables $U(k,j) = U_0(k,j)P(k,j)$. Provided the aperture is large enough (in our experiments, 100×100 pixels), the pixel-by-pixel correlation of the field allows us to consider such a field as virtually δ-correlated. A graphical representation of the normalised correlation function of the complex field amplitude is shown in Fig. 5.

The field of complex amplitudes is surrounded by sequences of zeros, which physically determine an opaque screen region, so that the entire field source matrix has 2000×2000 pixels. Such an increase in the number of the field source

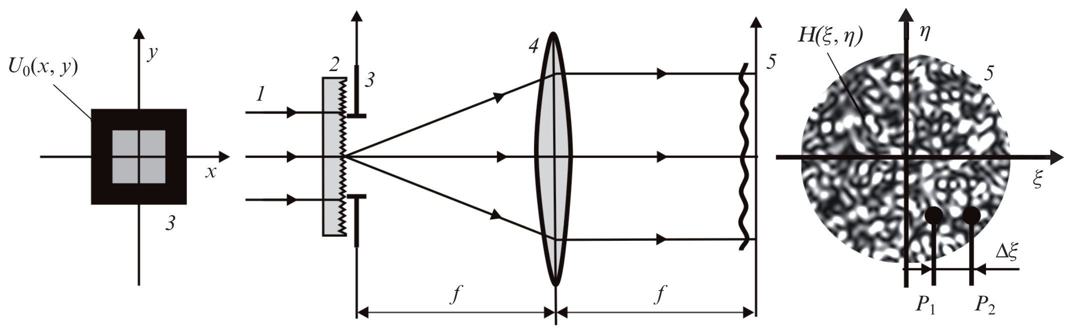

Figure 4. Schematic of a natural experiment to determine the phase difference at the speckle-field points in the far-field diffraction region: (*1*) illuminating parallel light beam; (*2*) scatterer; (*3*) aperture, i.e. an opaque screen with an opening; (*4*) lens; (*5*) speckle pattern in the far-field diffraction region.

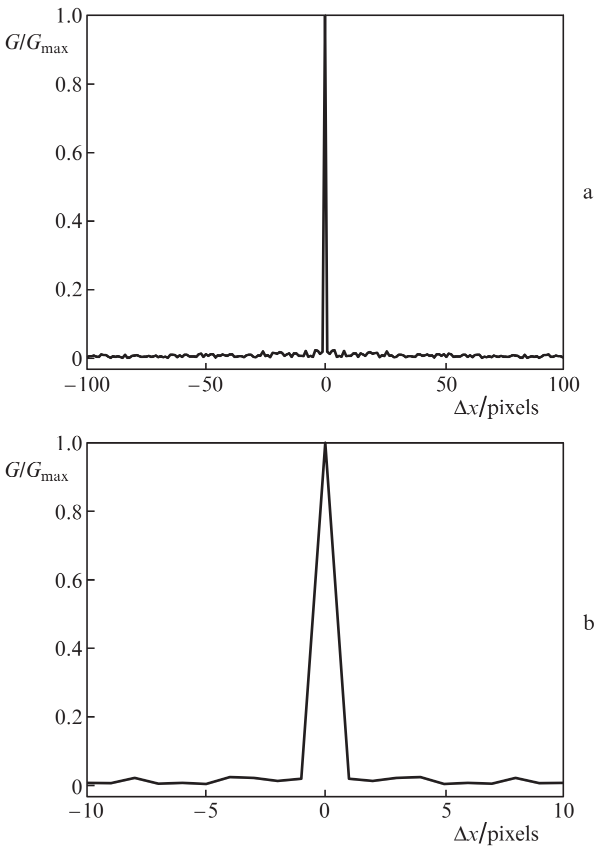

Figure 5. Normalised correlation function of the complex amplitude of the source field of the diffraction speckle-modulated field (a) and the central region of the correlation function (b).

pixels allows us to obtain a diffraction speckle-modulated field, wherein each speckle contains not a single pixel, as when using a matrix with aperture dimensions, but a sufficiently large number of pixels – in our case, for example, each speckle, for a square aperture, contains an average of 400 pixels.

The complex amplitude of the speckle-field in the far-field diffraction region is formed by means of the Fourier transform of the field source, using a fast Fourier transform algorithm. Thus, a matrix of complex amplitudes of the diffraction field, having a size of 2000 × 2000 pixels, is generated. The apertures of the speckle-field sources and the fragments of relevant simulated diffraction speckle patterns formed by such sources are presented in Fig. 1.

Random sampling of two points (P_1 and P_2) located in the diffraction speckle-field at a certain distance from each other along the ξ axis is performed, and the phase difference $\Delta\varphi$ of the fields at these points is numerically determined. The distance $\Delta\xi$ (on the scale of spatial frequency ξ) between the points P_1 and P_2 is defined relative to the width of a central maximum of the correlation function of the diffraction field, actually (from the physical viewpoint) relative to the minimal transverse size $\varepsilon_\perp$ of the speckles [2, 18].

Using a sample of N = 90000 values, histograms of the statistical distribution of the phase difference in the interval $[-\pi, \pi]$ are formed by partitioning this interval into m = 40 intervals. The envelopes of the histograms can be regarded as the curves describing the probability density functions of the phase difference $p(\Delta\varphi, \Delta\xi = \text{const})$ at a certain distance $\Delta\xi$ between the field points:

$$p(\Delta\varphi) = \Delta N(\Delta\varphi_i < \Delta\varphi < \Delta\varphi_{i+1})\frac{m}{2\pi N}, \qquad (3)$$

where $\Delta N(\Delta\varphi_i < \Delta\varphi < \Delta\varphi_{i+1})$ is the number of hits of the sample values into the phase difference range $[\Delta\varphi, \Delta\varphi_{i+1}]$. For different distances $\Delta\xi$, we have obtained histograms and, accordingly, spatial distributions of the phase difference $p(\Delta\varphi, \Delta\xi)$ for the speckle-field sources with apertures of various shapes.

Figure 6 shows the functions $p(\Delta\varphi, \Delta\xi)$ of the speckle-fields, obtained for the sources with apertures having the shape of a square ring (Fig. 1b) and an equilateral triangle (Fig. 1c). The outer side a of the triangle (Fig. 1a) amounts to 100 pixels, while its internal side b – to 80 pixels; for the triangular aperture (Fig. 1b), a = 100 pixels; the average size of the speckles in the diffraction field is 15–20 pixels for both apertures. The function $p(\Delta\varphi, \Delta\xi)$ in Fig. 6a demonstrates a significant nonuniformity of the density distribution of the phase difference $p(\Delta\varphi, \Delta\xi)$ for the distances $\Delta\xi$ between the field points, exceeding the transverse size of the field speckles, $\Delta\xi > \varepsilon_\perp$. The maxima of $p(\Delta\varphi, \Delta\xi)$ for the phase difference $\Delta\varphi = \pm\pi$ and $\Delta\xi \approx 1.5\varepsilon_\perp$ or $\Delta\xi \approx 3.5\varepsilon_\perp$ can be observed. From the physical standpoint, that means that the most probable value of the phase difference of the speckle-field in the neighbouring speckles is equal to π.

For a speckle field with constant-sign correlation properties, such as the field generated by the source with a triangular aperture, a virtually uniform distribution $p(\Delta\varphi, \Delta\xi)$ is observed

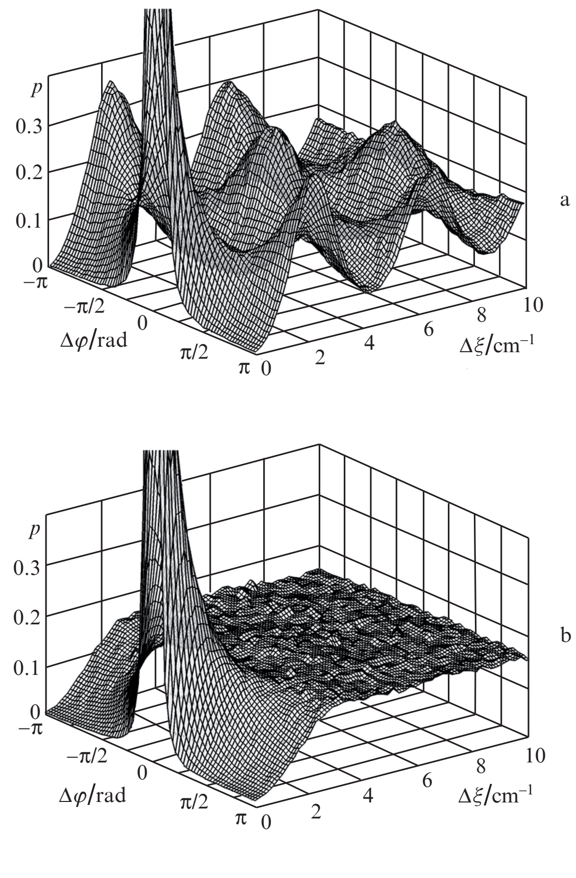

Figure 6. Spatial probability density function of the phase difference at two points of a diffraction speckle-field with the source aperture in the form of (a) square ring and (b) triangle.

for $\Delta\xi > \varepsilon_\perp$: $p(\Delta\varphi, \Delta\xi > \varepsilon_\perp) \approx 1/2\pi$ (Fig. 6b). From the physical viewpoint, that means that the phase difference in the neighbouring field speckles may take values in the entire interval $[-\pi, \pi]$ with equal probability.

The dependences of the probability density function of the phase difference on the parameters of the scatterer aperture manifest themselves most vividly in the cross sections for the fixed distances between the field points, $p(\Delta\varphi, \Delta\xi = \text{const})$. Figure 7 presents such dependences for the scatterer apertures in the form of a square and an annular square, with different ratios of the sides a/b for some typical distances between the points. From the physical viewpoint, these curves may be interpreted as follows.

When the distance $\Delta\xi$ between points P_1 and P_2 of the speckle-field is equal to half the average speckle size ($\Delta\xi \approx 0.5\varepsilon_\perp$), the probability for the points to fall into one and the same speckle attains its maximum; at the same time, the possibility for the points to fall into the neighbouring speckles is not excluded. In this case, nearly zero phase difference values are the most probable (Fig. 7a). When $\Delta\xi \approx \varepsilon_\perp$, the points fall within a single or neighbouring speckles with equal probability: in this case, a virtually uniform phase difference distribution is observed (Fig. 7b). At a distance $\Delta\xi \approx 1.5\varepsilon_\perp$, which is numerically equal to the coordinate of the first local maximum of the speckle-field correlation function, falling of the randomly sampled points into the neighbouring speckles is the most probable, though they may also fall into a single speckle. In this case, the values of the phase difference near $-\pi$ and π are the most probable (Fig. 7c). At a distance $\Delta\xi \approx 2.5\varepsilon_\perp$, numerically equal to the coordinate of the second local maximum of the correlation function of the speckle field, it is most probable that the randomly sampled points fall into the speckles through one; nevertheless, this does not exclude the possibility for them to fall into the neighbouring speckles and even into one and the same speckle. In this case, the values of the phase difference near zero are the most probable (Fig. 7d).

The results of numerical experiments show that the larger the absolute values of extremums of the correlation function of the complex amplitude of the speckle-field, the greater the maxima of the probability density function of the phase difference $p(\Delta\varphi, \Delta\xi)$ at two points of the speckle-field (Fig. 7). The greatest oscillation amplitudes of the field correlation function take place for annular apertures of the speckle-field source.

Figure 8 represents the probability density function of the phase difference $p(\Delta\varphi, \Delta\xi = \text{const})$ of the field sources with an aperture in the form of an annular square, when $\Delta\xi$ increases from $0.5\varepsilon_\perp$ up to $1.5\varepsilon_\perp$ (Fig. 8a) and from $1.5\varepsilon_\perp$ up to $2.5\varepsilon_\perp$ (Fig. 8b). In Fig. 8, with increasing $\Delta\xi$, the maxima of $p(\Delta\varphi, \Delta\xi)$ at $\Delta\varphi = 0$ decrease down to a nearly equiprobable distribution at $\Delta\xi \approx \varepsilon_\perp$, and then the maxima for $\Delta\varphi = \pm\pi$ increase with increasing $\Delta\xi$ up to $1.5\varepsilon_\perp$. In Fig. 8b, the maxima of $p(\Delta\varphi, \Delta\xi)$ for $\Delta\varphi = \pm\pi$ decrease down to a nearly equiprobable distribution at $\Delta\xi \approx 2\varepsilon_\perp$, and then the maxima of $p(\Delta\varphi, \Delta\xi)$ for $\Delta\varphi = 0$ at $\Delta\xi \approx 2.5\varepsilon_\perp$ increase.

The correlation function of the speckle-field generated by the source with an aperture in the form of a triangle has no alternating-sign oscillations (Fig. 3). An expressed maximum

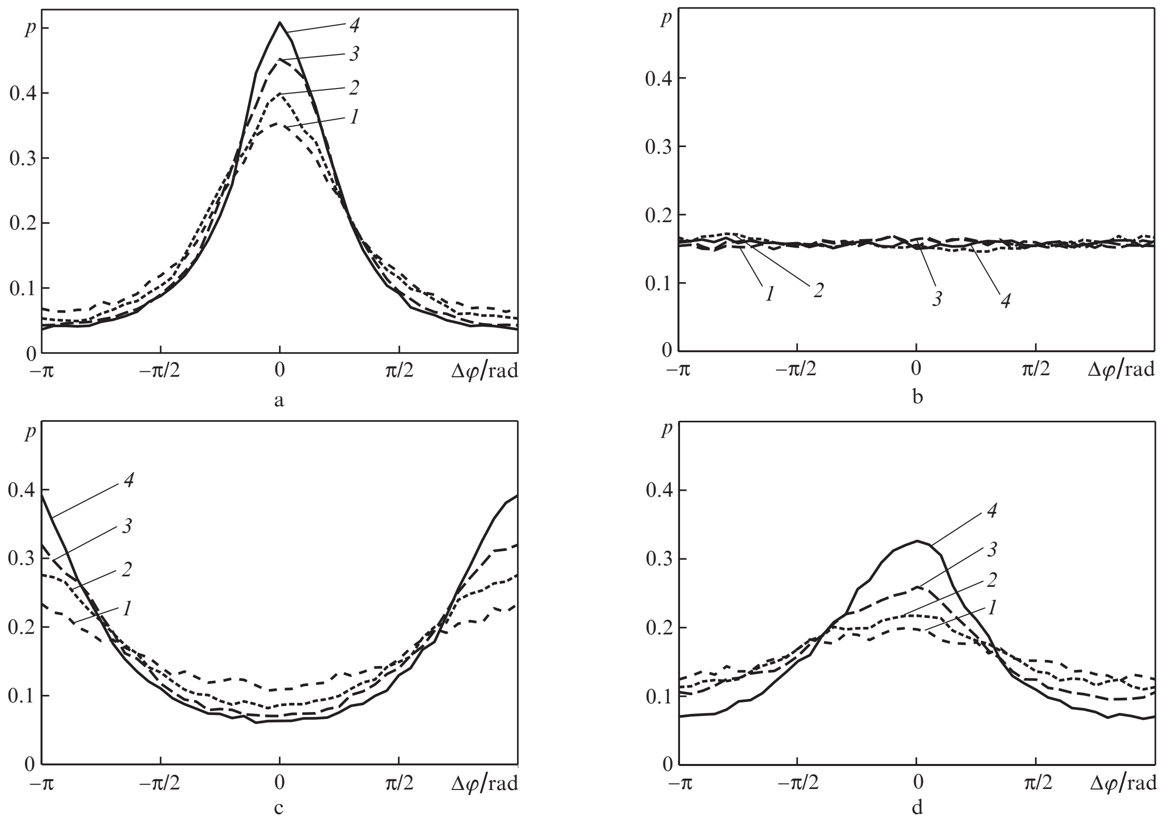

Figure 7. Probability density function of the phase difference at two points of the speckle-field for the sources with apertures in the form of a square (*1*) and an annular square with the ratio a/b equal to (*2*) 4, (*3*) 2 and (*4*) 4/3, for spacing $\Delta\xi$ between the speckle-field points, equal to half the coordinate of the first zero of correlation function of the speckle-field (a), coordinate of the first zero (b), coordinate of the first local maximum (c), and coordinate of the second local maximum (d).

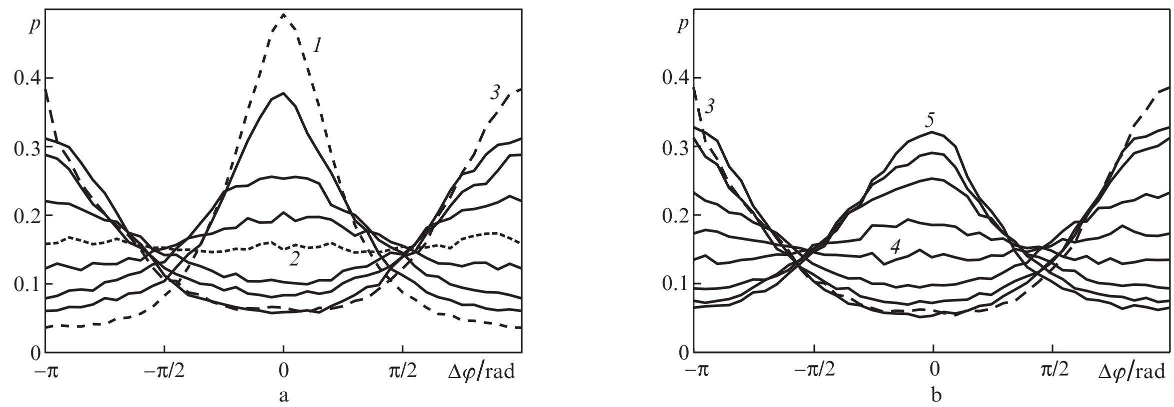

Figure 8. Probability density function of the phase difference at two speckle-field points for the sources with an aperture in the form of an annular square with $a/b = 4/3$ at $0.5\varepsilon_{\perp} \lesssim \Delta\xi \lesssim 1.5\varepsilon_{\perp}$ (a) and $1.5\varepsilon_{\perp} \lesssim \Delta\xi \lesssim 2.5\varepsilon_{\perp}$ (b). The ratio $\Delta\xi/\varepsilon_{\perp}$ is approximately equal to (*1*) 0.5, (*2*) 1, (*3*) 1.5, (*4*) 2 and (*5*) 2.5.

of the probability density function of the phase difference is observed near $\Delta\varphi = 0$ on the dependences $p(\Delta\varphi, \Delta\xi = \text{const})$ for the points falling into one and the same speckle (Fig. 9a). In other cases, a virtually uniform distribution of $\Delta\varphi$ holds true over the entire interval $[-\pi, \pi]$ (Figs 9b–d).

In the case the aperture has a shape of an annular triangle, small alternating-sign oscillations of the correlation field function occur (Fig. 3). Therefore, the values of $p(\Delta\varphi, \Delta\xi)$ slightly increase near $\Delta\varphi = \pm\pi$ for the points falling into the neighbouring speckles (Fig. 9b). For the points falling into one speckle, we observe an expressed maximum near $\Delta\varphi = 0$ (Fig. 9a), while, in other cases, the distribution over the entire interval $[-\pi, \pi]$ turns out virtually uniform (Figs 9b–d). Similar to the case of a symmetric source aperture of the speckle-field, the smaller the annular region width, the greater the modulus of the first negative maximum of the autocorrelation function and relevant maximum for $\Delta\varphi = \pm\pi$ (Fig. 9c).

Figure 10 shows the behaviour of the probability density of the phase difference of the speckle-fields for the fixed values $\Delta\varphi = 0$ and π when increasing the distance $\Delta\xi$ between the points for the speckle-field source with an aperture in the form of a square and an annular square. The smaller the

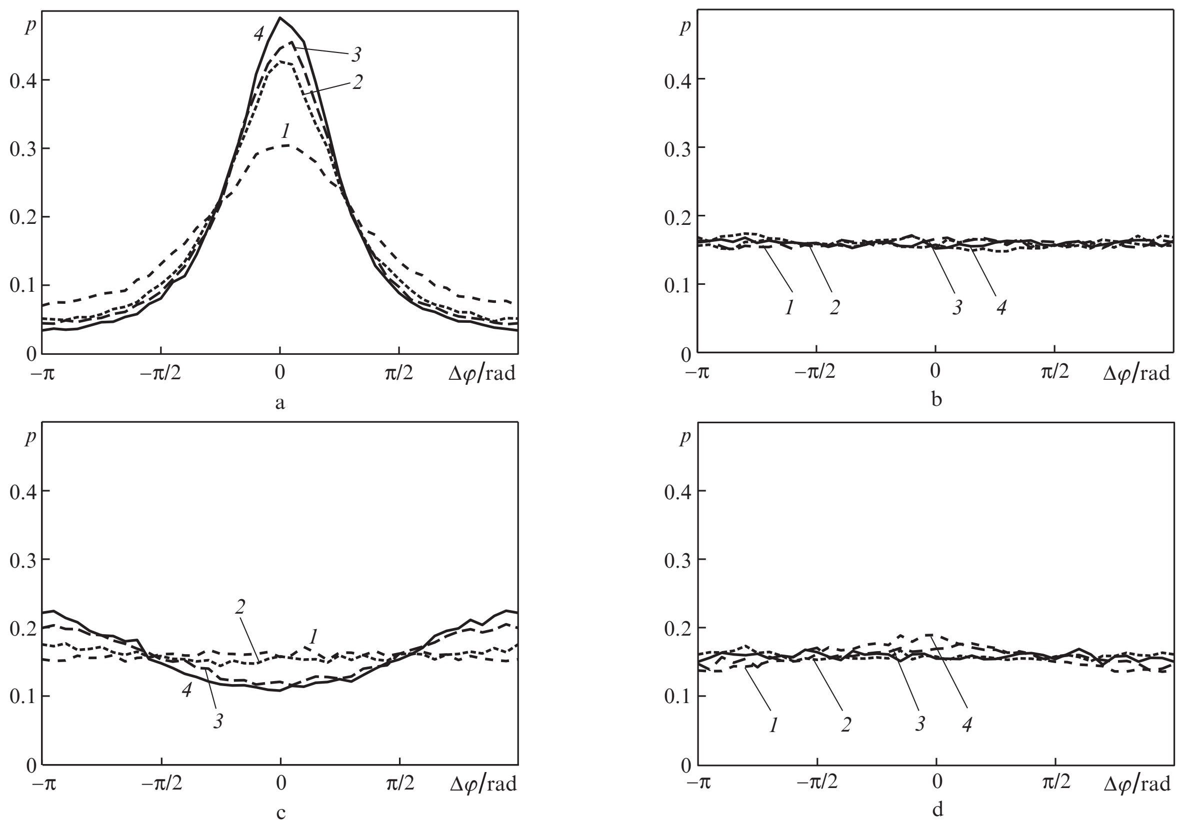

Figure 9. Probability density function of the phase difference at two speckle-field points for the sources with an apertures in the form of a triangle (*1*) and an annular triangle with the ratio a/b equal to (*2*) 4, (*3*) 2 and (*4*) 4/3. The ratio of the distance between the speckle-field points to the mean size $\Delta\xi/\varepsilon_{\perp}$ of the speckles is approximately equal to (a) 0.5, (b) 1, (c) 1.5 and (d) 2.5.

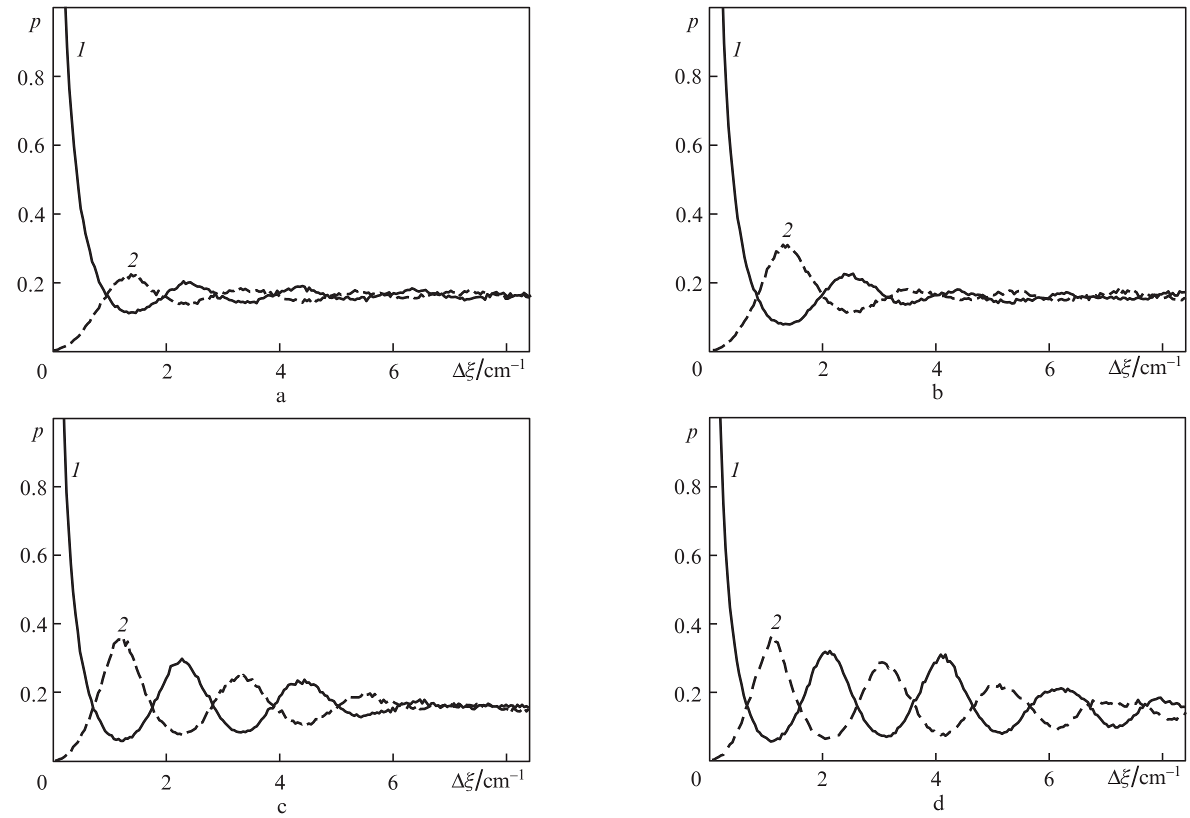

Figure 10. Probability density function of the phase difference at two speckle-field points with $\Delta\varphi = 0$ (*1*) and $\Delta\varphi = \pi$ (*2*) vs. distance $\Delta\xi$ between these points for the sources with apertures in the form of a square (a) and an annular square with the ratio *a*/*b* equal to (b) 2, (c) 4/3 and (d) 10/9.

annular region width on the source aperture, the greater the oscillation amplitude of the probability density function for the phase difference $\Delta\varphi = 0$ and π, and the slower the oscillations are damped with increasing $\Delta\xi$, which is an evidence of extension of the phase correlation region.

The results of numerical experiments (Figs 6–10) show that changing the sign of the correlation function of the complex amplitude of the speckle field is associated with a change in the sign of the complex field amplitude in a transition from one speckle to another. The greater the modulus of the first negative maximum of the correlation function, the greater the maxima of the probability density of the phase difference $p(\Delta\varphi)$ for$\Delta\varphi = \pm\pi$ and, consequently, the nonuniformity of the density distribution of the phase difference of the speckle-field.

4. Natural statistical experiment to determine the phase difference in the speckle-field

We have performed a statistical laboratory experiment to determine the phase difference of oscillations at two points of the speckle field, with computer processing of relevant interferograms, which provided the opportunity to operate with large sampling numbers – up to $N = 1000$ for each histogram. We have analysed four scatterer-restricting apertures such as the speckle-field source: square, annular square, triangle and annular triangle. For each aperture, statistics of changes in the phase difference at two speckle-field points for two characteristic distances between the points is determined. A phase difference between the oscillations arises in the interference experiment. The Young interferometer is the most suitable tool to determine the phase difference between two field points, since it allows observing interference of the waves outcoming from two openings in an opaque screen, upon which the field under study falls. If the screen openings are small compared to the transverse correlation length of the illuminating field, these quasi-point-like openings serve as the secondary sources of quasi-spherical waves. When the openings are illuminated by a spatially-coherent field, such as the laser speckle-modulated field, the interference of allocated waves is observed at any distance between the openings. However, the position of interference fringes depends on the phase difference of field oscillations in the openings. This circumstance makes it possible to determine the change in the phase difference of these oscillations by replacing the field realisation on the screen with openings and changing the spatial distribution of the phase of the illuminating field when changing the distance between the openings. Thus, the use of the Young interferometer offers an opportunity of performing a statistical experiment to determine the spatial probability density function of the phase difference at different field points versus the distance between them. This experiment assumes determination of the displacements of interference fringes relative to their period when replacing the realisations of the speckle-field incident on a screen with the openings.

Figure 11 presents a schematic of experimental determination of the phase difference at two points of the speckle-field with the Young interferometer. A beam from a laser (*1*) is reflected from a mirror (*2*), is expanded by means of a microlens (*3*), is collimated by a lens (*4*), and then passes through another lens (*5*) restricted by an aperture (*6*). The distance z_0 from aperture *6* to the screen with two point-like apertures (*8*) is much larger than the aperture size. The aperture's external size *a* is about 5 mm (the ratio *a*/*b* of the annular aperture sizes is equal to 2); the distance z_0 is about 1500 mm. Thus, we may assume that the screen with openings, on which the speckle-field falls, is located in the far-field diffraction region. In this experiment, we employed linearly polarised radiation from a He–Ne laser (the power of 25 mW power, the wavelength of 0.63 μm) and a digital camera (CMOS sensor, 5.7 mm × 4.28, 2592 × 1944 pixels).

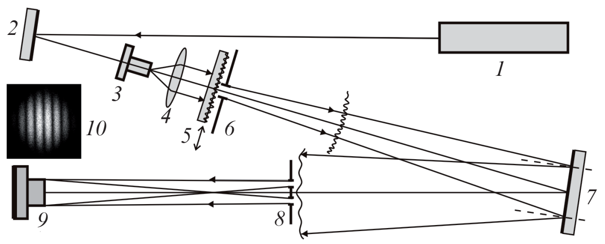

Figure 11. Schematic of the experiment on determination of the phase difference at two speckle-field points using the Young interferometer: (*1*) laser; (*2*, *7*) mirrors; (*3*) micro-objective, (*4*) lens; (*5*) scatterer; (*6*) aperture; (*8*) screen with two point-like apertures; (*9*) digital camera; (*10*) image of interference fringes on the matrix of the digital camera.

In our experiment, the distance $\Delta\xi$ between the screen openings remains constant ($\Delta\xi = 0.5$ mm), while the speckle size $\varepsilon_\perp$ is varied by changing the distance z_0 from the lens to the screen. Accordingly, the ratio $\Delta\xi/\varepsilon_\perp$, which constitutes 1.5 and 2.5 in the experiment, is also changed. The interference fringe pattern is formed on the digital camera matrix (Fig. 12), position of which depends on the phase difference $\Delta\varphi$ of the field in the apertures of the screen (*8*). When displacing lens *5* transversely by a value exceeding the aperture size, a complete replacement of the speckle-field realisation on the screen surface occurs. Variation in the field phase difference in the screen openings is determined from the transversal shift $\Delta x'$ of interference fringes in fractions of their period Λ:

$$\Delta\varphi = 2\pi\Delta x'/\Lambda. \quad (4)$$

The fringe shift $\Delta x'$ for each image of the interference pattern relative to the position of fringes in a reference image is determined by means of computer image processing of interference patterns as the displacement of the central peak of cross-correlation functions of the reference and current images of interference fringes relative to the position of the central peak of the autocorrelation function of the intensity distribution in the reference image.

The histograms presented in Fig. 13 are constructed on the basis of statistical data for the phase difference $\Delta\varphi$. The histograms in Figs 13a–d show a distinct nonuniformity of the probability density function of the phase difference at two points of the speckle field for the sources with apertures in the form of a square and, especially, in the form of an annular square. For the sources with such apertures, as indicated above, the speckle-field correlation function possesses local extremums being sufficiently pronounced (see Fig. 2). The greater those extremums in modulus, the greater the maxima of the probability density function of the phase difference, as can be seen from Fig. 13 for the case of an annular square aperture. At $\Delta\xi \approx 1.5\varepsilon_\perp$, when the Young interferometer openings with maximal probability correspond to the neighbouring speckles, a maximum of the probability density function of the phase difference is observed at $\Delta\varphi = \pi$. At $\Delta\xi \approx 2.5\varepsilon_\perp$, when, with maximal probability, the speckles fall through one into the screen openings, the maximum is attained at $\Delta\varphi = 0$.

The histograms in Figs 13a–d demonstrate a nearly jumpwise increase in the maxima near $\Delta\varphi = 0$, π, and a nearly uniform phase difference distribution in the rest of the interval. This can be explained by the fact that, in the natural statistical experiment, when changing the speckle field realisation, only bright and clear images of interference fringes have been selected. In these cases, the openings in the Young interferometer screen fall either into a single speckle, or the neighbouring speckles, or the speckles through one, and it is most probable that the phase difference herewith equals π or zero. In the realisation of the conditions $\Delta\xi \approx 1.5\varepsilon_\perp$ by means of increasing the distance z_0, the field's mean intensity decreases, and the images of interference fringes in diffraction halo become less bright than those at $\Delta\xi \approx 2.5\varepsilon_\perp$, which results in a lesser number of recorded 'good' images.

The field correlation function generated by a scatterer with an asymmetric aperture (in particular, having the form of a triangle) has no alternating-sign oscillations, while in the case of an annular triangle, the field correlation function undergoes sign-alternating oscillations of small amplitude. Therefore, the speckle-fields generated by the scatterers with such apertures are expected to have a nearly uniform probability density function of the phase difference. The results of the natural experiments presented in Figs 13e–h confirm this assumption as applied to the sources with asymmetric apertures.

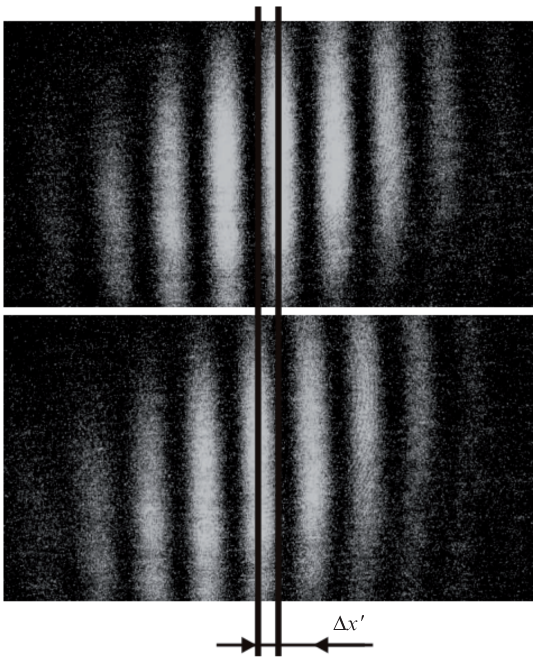

Figure 12. Displacement $\Delta x'$ of interference fringes in the diffraction halo when changing the speckle-field realisation. The period of interference fringes on the camera matrix is $\Lambda \approx 0.45$ mm (~200 pixels).

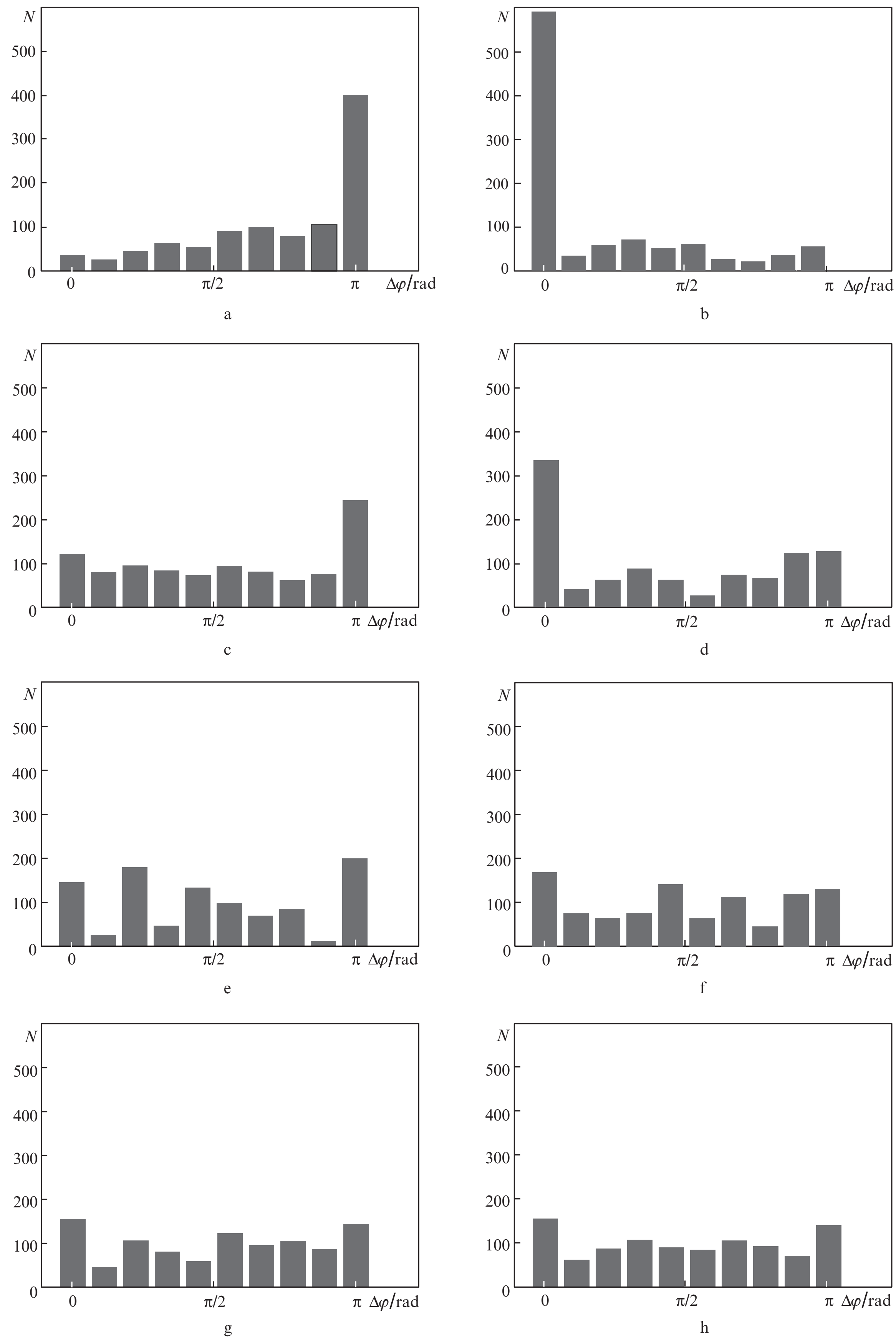

Figure 13. Histograms of the probability density function of the phase difference $\Delta\varphi$ at two points of the speckle-field generated by a source with the aperture in the form of (a, b) annular square, (c, d) square, (e, f) annular triangle and (g, h) triangle. The distance $\Delta\xi$ between the apertures in the Young interferometer screen is approximately equal to (a, c, e, g) $1.5\varepsilon_{\perp}$ and (b, d, f, h) $2.5\varepsilon_{\perp}$.

5. Conclusions

The nonuniformity of the statistical distribution of the phase difference in a developed speckle-field with the most probable $\Delta\varphi$ values equal to 0 and $\pm\pi$, depending on the distance between the field's points at which the phase difference of oscillations is determined, is conditioned by peculiarities of transverse correlation properties of the fields. Such a nonuniformity of the probability density function of the phase difference $p(\Delta\varphi)$ is observed within the speckle field correlation range, the transverse correlation properties of which are determined by the oscillating, alternating-sign function of the field's transverse correlation. Similar field correlation properties arise when a scatterer with a symmetric aperture is used as the speckle-field source. Moreover, these properties manifest themselves in a significantly greater degree when a symmetric structured aperture is used, in particular, an annular square aperture. In this case, the spatial correlation function of the field undergoes oscillations of a relatively high amplitude and, as a consequence, fairly large maxima in the probability density function of the phase difference $p(\Delta\varphi)$ at $\Delta\varphi = \pm\pi$ are observed if the distance between the points coincides with the oscillation intervals of the correlation function. Under these conditions, there is a nonuniform, oscillating in space, probability density function of the speckle-field phase difference. The nonuniformity of $p(\Delta\varphi)$ is observed within the region of the transverse correlation of the speckle-field, where oscillations of the complex field amplitude remain noticeable. Outside that region, the distribution of $p(\Delta\varphi)$ becomes virtually uniform.

It is commonly accepted that the separate speckles in the spatial intensity distribution of a speckle-modulated field (in the speckle pattern) can be considered as the region of the field correlation. The results obtained in this work show that the region of the field correlation has considerably larger limits. This especially applies to the speckle-fields formed by means of the scatterers with structured apertures. The size of speckles in the transverse intensity distribution in the speckle pattern is determined by the width of the central maximum of the field correlation function. However, significant correlations may still persist in the speckle-field beyond the limits of that maximum, which is manifested in the nonuniformity of the distribution $p(\Delta\varphi)$.

The most probable phase difference $\Delta\varphi = \pm\pi$ of the field in the neighbouring speckles of the diffraction zone may, in some cases, allow reconstruction of the phase information about the object field, which has been lost when recording the speckle-field intensity. As shown in [21–23], this fact can be employed to restore the image of a scattering object by recording the diffraction field intensity. A knowledge on statistical properties of the phase difference in the neighbouring speckles of the scattered field may also be of practical importance in laser interferometry, in particular, for evaluation of the statistical parameters of signals from laser speckle-interferometers during an analysis of the micro-displacements of scattering surfaces when a few speckles of a scattered object field fall into the photodetector aperture. The statistical regularities of the phase distributions, revealed in this work, may also be used to study the impact of the speckles on operation of wavefront sensors.

References

1. Goodman J.W. *Speckle Phenomena in Optics: Theory and Applications* (Englewood: Roberts & Company Publ., 2006).
2. Goodman J.W. In: *Laser Speckle and Related Phenomena.* Ed. by J.C. Dainty (Berlin: Springer-Verlag, 1975) p. 9.
3. Franson M. *Laser Speckle and Applications in Optics* (New York: Acad. Press, 1979; Moscow: Mir, 1980).
4. Jones R., Wykes C. *Holographic and Speckle Interferometry. A Discussion of the Theory, Practice and Application of the Techniques* (Cambridge: Cambridge University Press, 1983; Moscow: Mir, 1986).
5. Klimenko I.S. *Golographiya sfokusirovannykh izobrajenii i spekl-interferometriya* (Holography of Focused Images and Speckle Interferometry) (Moscow: Nauka, 1985).
6. Badalyan N.P., Kiiko V.V., Kislov V.I., Kozlov A.B. *Kvantovaya Elektron.*, **38**, 477 (2008) [*Quantum Electron.*, **38**, 477 (2008)].
7. Ivanov A.P., Katsev I.L. *Kvantovaya Elektron.*, **35**, 670 (2005) [*Quantum Electron.*, **35**, 670 (2005)].
8. Collier R., Burckhardt C.B., Lin L. *Optical Holography* (New York: Acad. Press, 1971; Moscow: Mir, 1973).
9. Schnars U., Juptner W. *Digital Holography* (Berlin: Springer-Verlag, 2004).
10. Rezchikov A.F., Ryabukho V.P. *Probl. Mashinostr. Nadezn. Mashin*, **1**, 68 (2010) [*Journal of Machinery Manufacture and Reliability*, **39** (1), 56 (2010)].
11. Kul'chin Yu.N., Vitrik O.B., Lantsov A.D. *Kvantovaya Elektron.*, **36**, 339 (2006) [*Quantum Electron.*, **36**, 339 (2006)].
12. Labeyrie A. *Ann. Rev. Astron. Astrophys.*, **16**, 77 (1978).
13. Martinache F. *J. Opt. A: Pure Appl. Opt.*, **6**, 216 (2004).
14. Larichev A.V., Ivanov P.V., Iroshnikov N.G., Shmal'gauzen V.I. *Kvantovaya Elektron.*, **31**, 1108 (2001) [*Quantum Electron.*, **31**, 1108 (2001)].
15. Trisnadi J.I. *Proc. SPIE Int. Soc. Opt. Eng.*, **4657**, 131 (2002).
16. Yurlov V., Lapchuk A., Yun S., Song J., Yeo I., Yang H., An S. *Appl. Opt.*, **48**, 80 (2009).
17. Svet V.D. *Open J. Biophys.*, **3**, 165 (2013).
18. Goodman J.W. *Statistical Optics* (New York: John Willey & Sons, Inc., 1985; Moscow: Mir, 1988).
19. Uozumi J., Asakura T. *Appl. Opt.*, **20**, 1454 (1981).
20. Kadono H., Takai N., Asakura T. *J. Opt. Soc. Am. A*, **3**, 1080 (1986).
21. Gorbatenko B.B., Ryabukho V.P., Maksimova L.A. *Opt. Spektrosk.*, **101**, 861 (2006).
22. Gorbatenko B.B., Maksimova L.A., Ryabukho V.P., Norov Yu.V. *Komp'yuternaya Optika*, **31**, 26 (2007).
23. Gorbatenko B.B., Maksimova L.A., Ryabukho V.P. *Opt. Spektrosk.*, **106**, 323 (2009).
24. Maksimova L.A., Mysina N.Yu., Gorbatenko B.B., Ryabukho V.P. *Proc. SPIE Int. Soc. Opt. Eng*, **8699**, 869910 (2013).
25. Mysina N.Yu., Maksimova L.A., Gorbatenko B.B., Ryabukho V.P. *Komp'yuternaya Optika*, **37**, 451 (2013).
26. Born M., Wolf E. *Principles of Optics* (London: Pergamon Press, 1959; Moscow: Nauka, 1973).
27. Goodman J.W. *Introduction to Fourier Optics* (New York: McGraw-Hill, 1968; Moscow: Mir, 1970).
28. Klimenko I.S., Ryabukho V.P., Feduleev B.V. *Zh. Tekh. Fiz.*, **55**, 1338 (1985).